Original Article

Pemafibrate, a PPAR alpha agonist, attenuates neointima formation after vascular injury in mice fed normal chow and a high-fat diet

Tsuyoshi Horikawa (thorikawa@fukuoka-u.ac.jp)[1], Takako Kawanami (namikawa9@fukuoka-u.ac.jp)[1], Yuriko Hamaguchi (yurikoh@fukuoka-u.ac.jp)[1], Yuki Tanaka (yfujimura@fukuoka-u.ac.jp)[1], Shotaro Kita (shotarokita1412@outlook.jp)[1], Ryutaro Ryorin (dustbox6396@hotmail.co.jp)[1], Yuichi Takashi (y.takashi.si@fukuoka-u.ac.jp)[1], Hiroyuki Takahashi (htakahashi@fukuoka-u.ac.jp)[1], Makito Tanabe (mtanabe@live.jp)[1], Toshihiko Yanase (t-yanase@seiwakai-hp.jp)[2], Daiji Kawanami (kawanami@fukuoka-u.ac.jp)[1], Takashi Nomiyama (tnomiyama@iuhw.ac.jp)[3]*

[1]Department of Endocrinology and Diabetes Mellitus, School of Medicine, Fukuoka University, Fukuoka, Japan

[2]Muta Hospital, Fukuoka, Japan

[3] Department of Diabetes, Metabolism and Endocrinology, International University of Health and Welfare Ichikawa Hospital
Department of Diabetes, Metabolism and Endocrinology, IUHW, School of Medicine, Chiba, Japan

*__Correspondence__: Takashi Nomiyama MD, PhD,
Department of Diabetes, Metabolism and Endocrinology, International University of Health and Welfare Ichikawa Hospital

, 6-1-14, Kounodai, Ichikawa, Chiba, Japan 272-0827

Tel: +81-47-375-1111

ABSTRACT

Recently, the prevention of cardiovascular events has become one of the most important aims of diabetes care. Peroxisome proliferator-activated receptor (PPAR) agonists have been reported to have vascular protective effects. Here, we examined whether pemafibrate, a selective PPAR alpha agonist, attenuated neointima formation after vascular injury and vascular smooth muscle cell (VSMC) proliferation. We performed endothelial denudation injury in mice treated with a high-fat diet (HFD) or normal chow. Orally administered pemafibrate significantly attenuated neointima formation after vascular injury in HFD and normal chow mice. Interestingly, pemafibrate increased the serum fibroblast growth factor 21 concentration and decreased serum insulin concentrations in HFD mice. In addition, body weight was slightly but significantly decreased by pemafibrate in HFD mice. Pemafibrate, but not bezafibrate, attenuated VSMC proliferation *in vitro.* The knockdown of PPAR alpha abolished the anti-VSMC proliferation effect of pemafibrate. BrdU assay results revealed that pemafibrate dose-dependently inhibited DNA synthesis in VSMCs. Flow cytometry analysis demonstrated that G1-to-S phase cell cycle transition was significantly inhibited by pemafibrate. Pemafibrate attenuated

serum-induced cyclin D1 expression in VSMCs. However, apoptosis was not induced by pemafibrate as assessed by the TUNEL assay. Similar to the *in vitro* data, VSMC proliferation was also decreased by pemafibrate in mice. These data suggest that pemafibrate attenuates neointima formation after vascular injury and VSMC proliferation by inhibiting cell cycle progression.

Keywords: diabetes mellitus, PPAR alpha agonist, cyclin d1, neointima formation, VSMC proliferation

Highlights

Pemafibrate attenuates neointima formation in mice fed normal chow and a high-fat diet.

Pemafibrate attenuates VSMC proliferation *in vitro*.

Pemafibrate attenuates cyclin D1 expression and DNA synthesis in VSMCs.

Introduction

Cardiovascular events (CVEs) are one of the most critical vascular complications in patients with type 2 diabetes mellitus (T2DM). Accordingly, large scale clinical trials investigating CVE reduction using novel anti-diabetic agents have provided profound results for diabetes care [1]. In addition to primary CVEs, restenosis after coronary angioplasty remains a critical problem for patients with T2DM [2]. Guidewire-induced endothelial denudation injury has been established as an experimental mouse model for restenosis and vascular thickening after coronary angioplasty or vascular injury [3]. Importantly, the pathogenesis of vascular thickening caused by wire injury reflects vascular smooth muscle cell (VSMC) proliferation after the phenotype switching of VSMCs [4]. Previously, we demonstrated that anti-diabetic agents, including glucagon-like peptide-1 (GLP-1) receptor agonist [5], dipeptidyl peptidase-4 (DPP-4) inhibitor [6], and sodium-glucose cotransporter 2 (SGLT2) inhibitor [7], attenuated neointima formation after vascular injury and VSMC proliferation. VSMC proliferation and phenotype switching are precisely regulated by nuclear receptors. We previously reported that nuclear orphan receptor NR4A neuron-derived orphan receptor1 (NOR1)

plays an important role in VSMC proliferation and neointima formation after vascular injury [8, 9]. Among nuclear orphan receptors, drugs targeting peroxisome proliferator-activated receptor (PPAR) alpha are clinically available for the treatment of hypertriglyceridemia, which is a residual risk for CVEs in patients with obesity and T2DM [10]. Pemafibrate (K-877) is a PPAR alpha agonist with a highly selective binding affinity to PPAR alpha compared with other agonists [11]. In the present study, we examined whether pemafibrate attenuated neointima formation in mice fed normal chow and a high-fat diet (HFD) and VSMC proliferation *in vitro*.

Materials and Methods

Animals

All study protocol and experiments were reviewed and approved by the Animal Care and Use Committee of Fukuoka University (Approval number 1705050). The study conformed to the *Guide for the Care and Use of Laboratory Animals* published by the US National Institutes of Health (NIH Publication No. 85-23, revised 1996). Four-week-old male C57BL/6 mice were purchased from Oriental Yeast (Tokyo, Japan). All mice were housed as previously described [7]. Water

was available *ad libitum*. Mice were divided into the following treatment groups: normal chow-control (n = 10), normal chow-pemafibrate (n = 10), HFD-control (n =10), and HFD-pemafibrate (n = 10). Pemafibrate was kindly provided by the Kowa Company, Ltd. (Tokyo, Japan). Control mice were fed normal chow (22.6% protein, 53.8% carbohydrate, 5.6% fat, 6.6% minerals, a vitamin mixture, and 3.3% fiber; 356 kcal/100 g) or HFD (20% protein, 20% carbohydrate, 60.0% fat, D12492, Research Diet) with methyl cellulose (vehicle control) or pemafibrate, at 6 weeks of age. Pemafibrate was dissolved in methyl cellulose, diluted with water, and administered to the relevant experimental groups (0.1 mg/kg/day). The animal room had a 12-h light/dark cycle, constant temperature (22 ± 1°C), and relative humidity of 55 ± 5% throughout the experimental period. Endothelial denudation injuries were induced in the left femoral artery at 8 weeks of age, followed by the evaluation of neointima formation at 12 weeks of age.

Guidewire-induced endothelial denudation injury

A femoral artery endothelial denudation injury was established in mice at 6 weeks of age as described previously [5-7, 9]. Mice were euthanized at 12 weeks of age, and femoral arteries were isolated for analysis.

Tissue preparation and morphometry

Following sacrifice, mice were perfused via a cannula in the left ventricle with phosphate-buffered saline for 5 min, followed by 4% paraformaldehyde for 30 min at 100 cm H_2O. The femoral arteries were embedded in paraffin, cut into 5-μm sections, and prepared for Elastica van Gieson staining. Serial sections were evaluated using an Elastica van Gieson stain kit (HT25A-1KT; Sigma-Aldrich, Tokyo, Japan) to visualize the internal elastic lamina as described previously [5-7]. Specimens were viewed under a BZ9000 microscope (Keyence, Tokyo, Japan). The intimal and medial areas were measured by computerized morphometry using a BZ-II analyzer (Keyence). Intimal hyperplasia was defined as described previously [5-7]. The medial area represents the area between external and internal elastic laminas. The intima-to-media ratio was calculated as the intimal area divided by the media area as described previously [5-7].

Immunohistochemistry

Paraffin sections were incubated with a Cy-3-conjugated α-smooth muscle actin antibody (C6198, Sigma Aldrich). Serial sections were incubated with an anti-

PCNA antibody (#sc-56, Santa Cruz) and subsequently incubated with an Alexa Fluor 546 goat anti-mouse IgG secondary antibody (#A-11030, Thermo Fisher Scientific). Sections were counterstained with DAPI and visualized by confocal microscopy.

Laboratory data

Blood samples were collected at euthanasia. The plasma glucose concentration was measured by a Glutest Neo Super device (Sanwa Chemical Co., Kanagawa, Japan). Insulin concentrations in mouse serum were measured using the Ultra Sensitive Mouse Insulin ELISA Kit (Morinaga Institute of Biological Science, Inc. Kanagawa, Japan) according to the manufacturer's protocol. Fibroblast growth factor 21 (FGF21) concentrations in mouse serum were measured using an FGF21 Mouse/Rat ELISA Kit (RD291108200R, BioVendor, Karasek, Czech Republic) according to the manufacturer's protocol. Lipid profiles were determined by a local laboratory (Skylight Biotech, Tokyo, Japan).

Cell culture

Rat aortic smooth muscle cells (RASMCs) were purchased from Lonza (Allendale, NJ, USA) and maintained in DMEM/Ham's F-12 (042-30555, Wako, Osaka, Japan) supplemented with 10% fetal bovine serum (FBS) and 1% penicillin/streptomycin. Passages three and six cells were used between for experiments, and individual experiments were repeated at least three times with different cell preparations.

Proliferation assay

Cell proliferation assays were performed as described previously [6, 7] with minor modifications. Briefly, RASMCs were seeded in 12-well tissue culture plates and maintained in complete media with or without 1–1000 nM pemafibrate or 100–500 μM bezafibrate (#022-16091, Fujifilm Wako Chemicals, Osaka, Japan). Cell proliferation was analyzed from 0 to 72 h by cell counting using a hemocytometer.

Small interfering RNA (siRNA) knockdown of *PPAR alpha* expression and cell proliferation assay

To knockdown *PPAR alpha*, we used an order-designed siRNA (Theoria Science, Tokyo, Japan) targeting rat *PPAR alpha*. We used negative control

siRNA from the same company, as a conrol. For transfection, RASMCs were plated at 2×10^5 cells/well in six-well plates and transfected with 10 nmol/l of siRNA targeting *PPAR alpha* or negative control siRNA using Lipofectamine RNAiMAX (Invitrogen, Carlsbad, CA, USA). Seventy-two hours after transfection, cells were subjected to the cell proliferation assay. Briefly, cells were detached and re-plated in 12-well tissue culture plates in complete media with or without 100 nM pemafibrate, or 100 μM bezafibrate. At 0–72 h after treatment, cells were collected and counted using a hemocytometer. The siRNA knockdown efficiency was confirmed by RT-PCR.

Bromodeoxyuridine (BrdU) assay

For evaluation of the cell proliferation of RASMCs, a BrdU incorporation assay was demonstrated using a Cell Proliferation ELISA kit (1647229; Roche Applied Science, Mannheim, Germany). RASMCs were cultured at 4000 cells/well in 96-well culture plates in complete media (n = 5). At 60%–70% confluence, cells were maintained in serum-free media for 24 h. At 12 h before serum stimulation, cells were treated with 0–1000 nM pemafibrate, or 0-1000μM bezafibrate and subsequently stimulated with 10% FBS for 48 h. A BrdU (10 μM) solution was

added during the last 2 h of incubation. Subsequently, the cells were dried and fixed, and cellular DNA was denatured with FixDenat solution (Roche Applied Science) for 30 min at room temperature. A peroxidase-conjugated mouse anti-BrdU monoclonal antibody (Roche Applied Science) was added to the culture plates, followed by incubation for 90 min at room temperature. Finally, a tetramethylbenzidine substrate was applied for 15 min at room temperature, and the absorbance of samples was measured using a microplate reader at 450–620 nm. Mean data were expressed as a ratio of the control (untreated) cell proliferation.

Cell cycle analysis using flow cytometry

RASMCs were seeded in 60-mm dishes at a density of 1×10^5 cells/ml. After growth to 60%–70% confluence and serum deprivation for 24 h, the cells were pretreated with 100 nM pemafibrate or dimethyl sulfoxide (DMSO) for 12 h and then stimulated with FBS for 24 h. Cell cycle analysis was performed using a Cycletest™ Plus DNA reagent kit (BD Biosciences, Franklin Lakes, NJ) following the manufacturer's instructions and BD FACSVerse (BD Biosciences, Franklin Lakes, NJ). Obtained data were analyzed by FlowJo (Tree Star, Inc., Ashland,

OR, USA).

Apoptosis assay

To label the nuclei of cells going into apoptosis, 1×10^5 RSMCs were plated on glass coverslips in Lab-Tek Chamber Slides (177380; Nunc, Thermo Scientific, Waltham, MA, USA) and maintained in complete media with 100 nM pemafibrate for 48 h. The cells were fixed in 4% paraformaldehyde for 25 min. Terminal deoxynucleotidyl transferase-mediated dUTP nick end labeling (TUNEL) was demonstrated using the DeadEnd Fluorometric TUNEL System (Promega, Madison, WI, USA) in accordance with the manufacturer's protocol. Cells treated with 1 U/100 µl RQ1 RNase-Free DNase (M6101; Promega) for 10 min were used as a positive control.

Western blot analysis

Western blotting was performed as described previously [13]. The following primary antibodies were used: Cyclin D1 (#2978; Cell Signaling Technology, Danvers, MA, USA) and β-actin (sc-47778; Santa Cruz Biotechnology, Santa Cruz, CA, USA).

Reverse transcription (RT) and quantitative real-time PCR

RT and quantitative real-time PCR were performed as described previously [13]. Each sample was analyzed in triplicate and normalized against *hypoxanthine phosphoribosyltransferase* (*HPRT*) mRNA expression. The primer sequences were as follows: rat *HPRT*, 5'-AGGACCTCTCGAAGTGTTGG-3' (forward), 5'-GATTCAACTTGCCGCTGTCT-3' (reverse); *rat Ppar alpha*, 5'-TGGCAATGCACTGAACATCG-3' (forward), 5'-GCAACAATCGCCTTTTGTC-3' (reverse); and rat *Ccnd1*, 5'-ATGCTGGTTTTTGCCTGGTG-3' (forward), 5'-AGCTAGCTGACCAAAAGTGC-3' (reverse).

Statistical analysis

Results are expressed as the mean ± SEM. All statistical analyses were performed using GraphPad Prism software (version 7.0; GraphPad Software, La Jolla, CA, USA). In experiments comparing multiple groups, differences were analyzed by an unpaired *t*-test or one-way or two-way ANOVA, followed by Sidak's *post-hoc* test as appropriate. $P < 0.05$ was considered statistically significant.

Results

Pemafibrate attenuates neointima formation in mice fed both normal chow and a HFD

To evaluate neointima formation after vascular injury by endothelial denudation, we performed elastic staining of the left femoral artery with injury extracted from mice maintained on a normal chow diet (Figure 1A). In the control vessel, obviously thickened neointima formation was observed. However, a much smaller neointima was observed in the vessels from pemafibrate-treated mice. Intima area and intima/media ratio measurements revealed that pemafibrate significantly reduced the intima/media ratio (Figure 1B). In the vascular injury of mice maintained on a HFD, pemafibrate reduced neointima formation (Figure 1C) and significantly reduced the intima/media ratio (Figure 1D).

Pemafibrate attenuates VSMC proliferation in mice fed both normal chow and a HFD

To confirm that pemafibrate attenuated neointima formation by inhibiting VSMC proliferation, we stained and counted VSMC numbers localized in the neointima

and media. As shown in Figure 2A, the neointima and media were occupied by VSMCs, and cell counting revealed that pemafibrate significantly attenuated VSMC numbers in the neointima and the intima/media ratio (Figure 2B). The same result was observed in HFD mice (Figure 2C, D). Laboratory data of mice are shown in Table 1. Compared with the normal chow group, body weight, serum insulin levels, LDL cholesterol, and HDL cholesterol were significantly increased, and VLDL cholesterol was significantly decreased in HFD mice. In HFD mice, the body weight and serum insulin level were significantly decreased by pemafibrate. Triglyceride and VLDL cholesterol were significantly decreased by pemafibrate in both groups. Interestingly, FGF21 was only detected in diabetic HFD mice and was significantly increased by pemafibrate.

Pemafibrate attenuates VSMC proliferation *in vitro*

To confirm that pemafibrate directly attenuated VSMC proliferation, we performed *in vitro* experiments using RASMCs. As shown in Figure 3A, pemafibrate significantly attenuated VSMC proliferation in a dose-dependent manner. However, the widely-used clinically available PPAR alpha agonist bezafibrate did not attenuate RASMC proliferation, and long-term incubation with bezafibrate

increased RASMC numbers, whereas pemafibrate decreased RASMC numbers (Figure 3B). The BrdU assay results revealed that pemafibrate but not bezafibrate attenuated RASMC proliferation by inhibiting DNA duplication dose-dependently (Figure 3C, D).

Pemafibrate attenuates VSMC proliferation via PPAR alpha activation

To confirm that pemafibrate attenuated RASMC proliferation via PPAR alpha activation, we knocked down PPAR alpha in RASMCs. As shown in Figure 4A, a significant reduction in cell proliferation induced by pemafibrate was observed in RASMCs treated with control siRNA, but the anti-proliferative effect of pemafibrate was completely abolished by knocking down PPAR alpha. However, bezafibrate did not decrease the number of RASCs treated by both the control and PPAR alpha siRNA (Figure 4B). To confirm the knockdown efficiency of PPAR alpha, we performed quantitative RT-PCR of *PPARalpha*. As shown in Figure 4C, *PPARalpha* expression was almost completely abolished in cells transfected with siRNA targeting *PPARalpha*.

Pemafibrate attenuates VSMC proliferation by inhibiting cyclin D1 expression and cell cycle progression but does not induce apoptosis

VSMC proliferation is mainly regulated by cell cycle progression, and therefore we performed flow cytometry analysis to determine cell cycle distribution. As shown in Figure 5A, pemafibrate attenuated the G0/G1-to-S phase transition induced by serum stimulation in RASMCs. However, pemafibrate did not induce apoptosis in RASMCs (Figure 5B). Cyclin D1 is an important cell cycle regulator in the G0/G1-to-S phase transition and is a target gene of PPAR alpha required for VSMC proliferation [14]. Next, we examined cyclin D1 expression. As shown in Figure 5C, cyclin D1 protein expression induced by serum stimulation was significantly decreased by pemafibrate. In addition, *cyclin D1* gene expression was significantly decreased by pemafibrate (Figure 5D).

Pemafibrate attenuates VSMC proliferation *in vivo*

To confirm the mechanism by which pemafibrate attenuates neointima formation and connect the data obtained from *in vitro* and *in vivo* experiments, we performed the immunohistochemistry of proliferation cell nuclear antigen (PCNA) using injured mice vessels. As shown in Figure 6, the proportion of PCNA-positive

proliferating VSMCs was significantly decreased by pemafibrate in both mice fed normal chow (Figure 6A, B) and a HFD (Figure 6C, D).

Discussion

Currently, the aim of treating patients with diabetes includes glucose-lowering and decreasing CVEs [1]. In addition to anti-diabetic agents, the vascular protective effects of lipid-lowering drugs, such as statins [15] and eicosapentaenoic acid [16], were demonstrated in patients with T2DM. However, the vascular protective effect of fibrates is not well understood either in the clinic or basic science research. In the present study, we investigated whether pemafibrate attenuated neointima formation in both mice fed normal chow and a HFD. Cell counting revealed that the inhibition of neointima formation by pemafibrate was related to the attenuation of VSMC proliferation. In HFD mice, body weight and serum insulin levels were significantly decreased by pemafibrate, suggesting pemafibrate improved insulin resistance and hyperinsulinemia. Because insulin is a proliferation stimulus for VSMCs, the reduction in serum insulin levels may be a mechanism by which pemafibrate decreased neointima formation after vascular injury. However, an insulin-independent mechanism may

also exist because pemafibrate decreased neointima formation in non-diabetic and non-hyperinsulinemic mice on a normal chow diet. Interestingly, serum FGF21 levels were increased by pemafibrate in HFD mice. In a previous study, pemafibrate increased serum FGF21 levels in humans [18] and *FGF21* gene expression in mice [19]. In addition, pemafibrate attenuated neovascularization by increasing FGF21 [20]. However, FGF21 was not part of the mechanism by which pemafibrate attenuated neointima formation because we did not observe an anti-proliferative effect of FGF21 in VSMC *in vitro* experiments (data not shown). Further studies of the vascular protective effect of FGF21 induced by pemafibrate are required. In the previous report, Lee et al. reported that the PPAR alpha agonist fenofibrate also reduced neointima formation after vascular injury [21]. In this report, they observed a 30%–40% reduction in neointima formation after vascular injury, which was greater than our present data. However, the animal model and drug dose were substantially different. Therefore, further experiments directly comparing the reduction in neointima formation by PPAR alpha agonists are required.

We also observed that pemafibrate attenuated VSMC proliferation *in vitro*, suggesting it directly attenuates VSMC proliferation independent of body weight

and serum insulin level reduction. Interestingly, another PPAR alpha agonist, bezafibrate, which is clinically available as a drug for hypertriglyceridemia, did not inhibit VSMC proliferation even at a higher dose compared with pemafibrate. This suggests that the vascular protective effect of pemafibrate is not a class effect of fibrates but a specific drug effect of pemafibrate. This might be a feature of the selective PPAR alpha modulator [19]. Furthermore, knocking down PPAR alpha confirmed that the molecular target of pemafibrate that attenuated VSMC proliferation was PPAR alpha. In the BrdU assay, >10 nM pemafibrate decreased DNA synthesis; however, the serum concentration of pemafibrate administered orally at a clinical dose is almost 3 nM (unpublished data by Kowa Company Ltd.), suggesting that our data might mirror clinical conditions. Compatible with our previous reports regarding the inhibition of VSMC proliferation [9, 22], pemafibrate attenuated VSMC proliferation by inhibiting G0/G1-to-S phase cell cycle transition. Furthermore, cyclin D was the target molecule and gene, similar to a previous report [14]. However, other reports suggested that the target of PPAR alpha in VSMCs was p16INKa [23] and that p16 and cyclin D1 correlated with VSMC biology [24]. Further experiments to elucidate the precise molecular mechanism by which pemafibrate attenuates VSMC proliferation are required. In

the present study, we observed that pemafibrate attenuated VSMC proliferation both *in vitro* and *in vivo*. These data suggested that the anti-proliferative effect could be a confirmative direct mechanism by which pemafibrate attenuates vascular diseases. There are some limitations to our VSMC experiments. We used only VSMC cultures because we focused on VSMC proliferation. However, the micro-artery does not include VSMCs. Accordingly, our experiments demonstrated the pathophysiology of the muscular artery. In addition, we cultured VSMCs in high glucose medium following the supplier's instruction and cell culture protocol. This did not precisely reproduce normal glucose tolerance conditions, and single-cell culture does not enable cell-cell interactions. Therefore, further elucidation is required. In addition to our study, previous reports demonstrated a vascular protective effect of pemafibrate using other vascular cells, such as endothelial cells [25] and macrophages [26], suggesting that this effect of pemafibrate is not cell-type specific.

In a previously reported clinical study, fenofibrate did not reduce CVEs in patients with T2DM and metabolic syndrome [27]. In addition, it was reported that fenofibrate was not associated with beneficial changes in carotid intima-media thickness in patients with T2DM [28]. Unfortunately, these data suggested that

the reduction in hypertriglyceridemia induced by fibrate did not exhibit a vascular protective effect, even if hypertriglyceridemia is the most critical risk factor for CVEs in Japanese patients with T2DM [29]. However, a clinical study investigating pemafibrate is currently ongoing [30]. Hopefully, we will observe CVE reduction by pemafibrate in patients with T2DM.

In conclusion, we report that the PPAR alpha agonist pemafibrate attenuates neointima formation in both mice fed by normal chow and HFD, and reduced VSMC proliferation by inhibiting cyclin D1 expression and cell cycle progression.

Acknowledgments

Pemafibrate was kindly provided by Kowa Company, Ltd. (Tokyo, Japan). We thank Edanz Group (https://en-author-services.edanzgroup.com/) for editing the English text of a draft of this manuscript.

References

[1] Acharya T, Deedwania P. Cardiovascular outcome trials of the newer anti-diabetic medications. Prog Cardiovasc Dis. 62 (2019) 342-348.

https://www.sciencedirect.com/science/article/pii/S0033062019301069?via%3Dihub

[2] Scheen AJ, Warzee F. Diabetes is still risk for restenosis after drug-eluting stent in coronary arteries. Diabetes Care. 27 (2004) 1840-1841. http://care.diabetesjournals.org/content/27/7/1840.long.

[3] Roque M, Fallon JT, Badimon JJ, et al. Mouse model of femoral artery denudation injury associated with the rapid accumulation of adhesion molecules on the luminal surface and recruitment of neutrophils. Arterioscler Thromb Vasc Biol. 20 (2000) 335-342. https://www.ahajournals.org/doi/10.1161/01.ATV.20.2.335.

[4] Frismantiene A, Philippova M, Eme P, Resink TJ. Smooth muscle cell-driven vascular diseases and molecular mechanisms of VSMC plasticity. Cell Signal. 52 (2018) 48-64. https://www.sciencedirect.com/science/article/pii/S0898656818302031?via%3Dihub#f0010.

[5] Goto H, Nomiyama T, Mita T, et al. Exendin-4, a glucagon-like peptide-1 receptor agonist, reduces intimal thickening after vascular injury. Biochem

Biophys Res Commun. 405 (2011) 79-84. https://www.sciencedirect.com/science/article/pii/S0006291X1002382X.

[6] Terawaki Y, Nomiyama T, Kawanami T, et al. Dipeptidyl peptidase-4 inhibitor linagliptin attenuates neointima formation after vascular injury. Cardiovasc Diabetol. 13 (2014) 154. https://cardiab.biomedcentral.com/articles/10.1186/s12933-014-0154-3.

[7] Takahashi T, Nomiyama T, Terawaki Y, et al. Combined treatment with DPP-4 inhibitor linagliptin and SGLT2 inhibitor empagliflozin attenuates neointima formation after vascular injury in diabetic mice. Biochem Biophys Rep. 18 (2019) 100640. https://www.sciencedirect.com/science/article/pii/S2405580818302668?via%3Dihub

[8] Nomiyama T, Nakamachi T, Gizard F, et al. The NR4A orphan nuclear receptor NOR1 is induced by platelet-derived growth factor and mediates vascular smooth muscle cell proliferation. J Biol Chem. 281 (2006) 33467-33476. http://www.jbc.org/content/281/44/33467.long

[9] Nomiyama T, Zhao Y, Gizard F, et al. Deficiency of the NR4A neuron-derived orphan receptor-1 attenuates neointima formation after vascular injury.

Circulation. 119 (2009) 577-586. https://www.ahajournals.org/doi/abs/10.1161/CIRCULATIONAHA.108.822056.

[10] Fruchart JC, Santos RD, Libby P. The selective peroxisome proliferator-activated receptor alpha modulator (SPPARMα) paradigm: conceptual framework and therapeutic potential. Cardiovasc Diabetol. 18 (2019) 71. https://doi.org/10.1186/s12933-019-0864-7

[11] Yamashita S, Masuda D, Matsuzawa Y. Pemafibrate, a new selective PPARα modulator: drug concept and its clinical applications for dyslipidemia and metabolic diseases. Curr Atheroscler Rep. 22 (2020) 5. https://link.springer.com/article/10.1007/s11883-020-0823-5

[12] Araki M, Nakagawa Y, Oishi A, et al. The peroxisome proliferator-activated receptor α (PPARα) agonist pemafibrate protects against diet-induced obesity in mice. Int J Mol Sci. 19 (2018) 2148. https://www.mdpi.com/1422-0067/19/7/2148

[13] Shigeoka T, Nomiyama T, Kawanami T, et al. Activation of glucagon-like peptide-1 receptor attenuates prostate cancer growth by inhibiting cell cycle progression. J Diabetes Investig. 2020, in press https://onlinelibrary.wiley.com/doi/full/10.1111/jdi.13247

[14] Zao Y, Liu Y, Jing Z, et al. N-oleoylethanolamide suppresses intimal hyperplasia after balloon injury in rats through AMPK/PPARa phathway. Biochem Biophys Res Commun. 496 (218) 415-421.

https://www.sciencedirect.com/science/article/pii/S0006291X18300159?via%3Dihub

[15] Tajima N, Kurata H, Nakata N, et al. Pravastatin reduces the risk for cardiovascular disease in Japanese hypercholesterolemic patinets with impaired fasting glucose or diabetes: diabetes subanalysis of the management of elevated cholesterol in the primary prevention group of adult Japanese (MEGA) study. Atherosclerosis. 199 (2008) 455-462.

https://www.sciencedirect.com/science/article/pii/S0021915008003663?via%3Dihub

[16] Oikawa S, Yokoyama M, Origasa H, et al. Suppressive effect of EPA on the incidence of coronary events in hypercholesterolemia with impaired glucose metabolism: sub-analysis of the Japan EPA lipid intervention study (JELIS). Atherosclerosis 206 (2009) 535-539.

https://www.sciencedirect.com/science/article/pii/S0021915009002408?via%3Dihub

[17] Breen DM, Giacca A. Effect of insulin on the vasculature. Curr Vasc Pharmacol. 9 (2011) 321-332.

http://www.eurekaselect.com/87935/article

[18] Fruchart JC. Pemafibrate (K-877), a novel selective peroxisome proliferator-activated receptor alpha modulator for management of atherogenic dyslipidemia. Cardiovasc Diabetol. 16 (2017) 214.

https://cardiab.biomedcentral.com/articles/10.1186/s12933-017-0602-y

[19] Sasaki Y, Raza-Iqbal S, Tanaka T, et al. Gene expression profiles induced by novel selective peroxisome proliferator activated receptor α modulator (SPPARMα) pemafibrate. In J Mol Sci. 20 (2019) 5682.

https://www.mdpi.com/1422-0067/20/22/5682/htm

[20] Tomita Y, Ozawa N, Miwa Y, et al. Pemafibrate prevents retinal pathological neovascularization by increasing FGF21 level in a murine oxygen-induced retinopathy model. Int J Mol Sci. 20 (2019) 5878.

https://www.mdpi.com/1422-0067/20/23/5878/htm

[21] Lee JJ, Yu JY, Zhang WY, et al. Inhibitory effect of fenofibrate on neointima hyperplasia via G0/G1 arrest of cell proliferation. Eur J Pharmacol. 650(2011)342-349.

https://www.sciencedirect.com/science/article/pii/S0014299910010733?via%3Dihub

[22]Takahashi H, Nomiyama T, Terawaki Y, et al. GLP-1 receptor agonist exendin-4 attenuates NR4A orphan receptor NOR1 expression in vascular smooth muscle cells. J Atheroscler Thromb. 26 (2019) 183-197. https://www.jstage.jst.go.jp/article/jat/26/2/26_43414/_article

[23] Gizard F, Amant C, Barbier O, et al. PPAR alpha inhibits vascular smooth muscle cell proliferation underlying intimal hyperplasia by inducing the tumor suppressor p16INK4a. J Clin Invest. 115 (2005) 3228-3238. https://www.jci.org/articles/view/22756

[24] Izzard TD, Taylor C, Birkett SD, et al. Mechanisms underlying maintenance of smooth muscle quiescence in rat aorta: role of the cyclin dependent kinases and their inhibitors. Cardiovasc Res. 53 (2002) 242-252. https://academic.oup.com/cardiovascres/article/53/1/242/432274

[25] Kawanishi H, Ohashi K, Ogawa H, et al. A novel selective PPARα modulator, pemafibrate promotes ischemia-induced revascularization through the eNOS-dependent mechanisms. PLOS ONE. (2020) https://journals.plos.org/plosone/article?id=10.1371/journal.pone.0235362

[26] Hennuyer N, Duplan I, Paquet C, et al. The novel selective PPARa modulator (SPPARMa) pemafibrate improves dyslipidemia enhances reverse cholesterol transport and decreases inflammation and atherosclerosis. Atherosclerosis. 249 (2016) 200-208. https://www.sciencedirect.com/science/article/pii/S0021915016300788?via%3Dihub

[27] Scott R, O'Brien R, Fulcher G, et al. Effects of fenofibrate treatment on cardiovascular disease risk in 9,795 individuals with type 2 diabetes and various complications of the metabolic syndrome. Diabetes Care. 32 (2019) 493-498. https://care.diabetesjournals.org/content/32/3/493.long

[28] Hiukka A, Westerbacka J, Leinonen ES, et al. Long-term effects of fenofibrate on carotid intima-media thickness and augmentation index in subjects with type 2 diabetes mellitus. J Am Coll Cardiol. 52 (2008) 2190-219. https://www.sciencedirect.com/science/article/pii/S0735109708036632?via%3Dihub

[29] Sone H, Tanaka S, Tanaka S, et al. Serum level of triglyceride is a potent risk factor compatible to LDL cholesterol for coronary heart disease in Japanese

patients with type 2 diabetes: subanalysis of the Japan Diabetes Complications Study (JDCS). J Clin Endocrinol Metab. 96 (2011) 3448-3456. https://academic.oup.com/jcem/article/96/11/3448/2834535

[30] Pradhan AD, Paynter NP, Everett BM, et al. Rationale and design of the pemafibrate o reduce cardiovascular outcomes by reducing triglycerides in patients with diabetes (PREMINENT) study. Am Heart J. 206 (2018) 80-93. https://www.sciencedirect.com/science/article/pii/S0002870318302801?via%3Dihub

Figure legends

Figure 1. Pemafibrate attenuates neointima formation after vascular injury in mice with or without a HFD.

Endothelial denudation injuries were induced in the left femoral artery of mice maintained with normal chow (A, B) or a HFD (C, D). (A, C) The left femoral artery with injury was evaluated by Elastica van Gieson staining to visualize the internal elastic lamina (magnification, ×200). (B, D) Intima areas and the intima/media

ratio (I/M ratio) were calculated for each group. Data are the mean ± SEM. Unpaired *t*-test was performed to calculate statistical significance (*$P < 0.05$ vs control).

Figure 2. Pemafibrate attenuates VSMC proliferation and migration after vascular injury in mice with or without a HFD.

Endothelial denudation injuries were induced in the left femoral artery of mice maintained on normal chow (A, B) or a HFD (C, D). (A, C) Sections were subjected to immunohistochemistry for α-SMA (red) and counterstained with DAPI to visualize nuclei (blue). Magnification, 630×. (B, D) Total DAPI count of the intima and the intima/media ratio (I/M ratio) were calculated for each group. Data are the mean ± SEM. Unpaired *t*-test was performed to calculate statistical significance (*$P < 0.05$ vs control).

Figure 3. Pemafibrate but not bezafibrate attenuates VSMC proliferation.

RASMCs were maintained in medium without FBS for 24 h. At 12 h before stimulation, control (DMSO), 1–1000 nM pemafibrate (A), or 100–500 μM bezafibrate and 100 nM pemafibrate (B) were added, and cells were

subsequently stimulated with 10% FBS. RASMCs were harvested, and cell proliferation was analyzed by cell counting using a hemocytometer. Data are the mean ± SEM. One-way ANOVA was performed to calculate statistical significance (**P < 0.01 vs control). RASMCs were maintained in medium without FBS for 24 h. At 12 h before stimulation, control (DMSO), 1–1000 nM pemafibrate (C), or 100–1000 μM bezafibrate was added. After 48 h stimulation, cells were harvested, and BrdU assays were performed to measure DNA synthesis. Data are expressed as a relative absorbance to 0 nM pemafibrate. One-way ANOVA was performed to calculate statistical significance (**P < 0.01 vs 0 nM).

Figure 4. Pemafibrate but not bezafibrate attenuates VSMC proliferation via PPAR alpha activation *in vitro*.

RASMCs were transfected with negative control duplexes (control) or *PPAR alpha* siRNA (SiPPAR) and maintained in media supplemented with 10% FBS and control DMSO (D) or 100 nM pemafibrate (indicated as K) (A) and 100 μM bezafibrate (indicated as B) (B). RASMCs were harvested, and cell proliferation was analyzed by cell counting using a hemocytometer. Data are the mean ± SEM. One-way ANOVA was performed to calculate statistical significance (**P < 0.01

vs DMSO). (C) Quantitative real-time RT-PCR of *PPARalpfa* was performed in RASMCs transfected with control siRNA (si-CT) or siRNA targeting *PPARalpha* (siPPARa). Gene expression was calculated by normalization to *HPRT*. An unpaired *t*-test was performed to calculate statistical significance (***P* < 0.01 vs si-CT, n=3).

Figure 5. Pemafibrate attenuates RASMC proliferation by reducing DNA synthesis but not by inducing apoptosis.

(A) Flow cytometric analysis was performed to determine the cell cycle distribution. Data represent the ratios of cells distributed in each phase to the mean total cell percentage ± SEM. The unpaired *t*-test was performed to calculate statistical significance. Black bar: before serum stimulation (n=3), gray bar: 24 h serum stimulation without pemafibrate (n=3), and white bar: 24 h serum stimulation with pemafibrate (n=3) (**P* < 0.05 vs 24 h serum stimulation without pemafibrate). (B) Apoptotic cells were detected by TUNEL staining. Images are representative of three independent experiments. (C) RASMCs were maintained in medium without FBS for 24 h. At 12 h before stimulation, control (DMSO) or 100 nM pemafibrate was added, and cells were subsequently stimulated with

10% FBS. After 24 h, cells were harvested, and western blotting of cyclin D1 was performed. Data are the mean ± SEM. Two-way ANOVA was performed to calculate statistical significance. (*P < 0.05 vs RASMCs without pemafibrate, n=3). (D) Quantitative real-time RT-PCR of *Cyclin D1* was performed in RASMCs in the presence or absence of pemafibrate. Gene expression was determined by normalization to *HPRT*. Two-way ANOVA was performed to calculate statistical significance (*P < 0.05, **P < 0.01 vs RASMCs without pemafibrate, n=3).

Figure 6. Pemafibrate attenuates VSMC proliferation *in vivo*.

Endothelial denudation injuries were induced in the left femoral artery of mice maintained on normal chow (A, B) or a HFD (C, D). (A, C) Sections were subjected to immunohistochemistry for PCNA (red) and counterstained with DAPI to visualize nuclei (blue). Magnification, 630×. (B, D) PCNA-positive cells were quantified by analyzing the fraction of stained cells to the total number of nuclei (n=5). Data are the mean ± SEM. An unpaired *t*-test was performed to calculate statistical significance (*P < 0.05 vs control).

Table 1. Laboratory data of mice after treatment with or without pemafibrate.

	Normal chow		High-fat diet	
	Control(*n*=8)	Pemafibrate(*n*=6)	Control(*n*=9)	Pemafibrate(*n*=6)
Body weight (g)	25.0 ± 0.4	25.6 ± 0.3	35.3 ± 0.8$^{\#\#}$	31.5 ± 0.7*
Blood glucose (mg/dl)	176.2 ± 4.2	193.2 ± 5.3	182.4 ± 8.0	184.4 ± 9.0
Insulin (ng/ml)	0.49 ± 0.10	0.45 ± 0.08	1.21 ± 0.14$^{\#\#}$	0.63 ± 0.10*
FGF21 (ng/ml)	ND	ND	0.21 ± 0.04	1.31 ± 0.13**
Triglyceride (mg/dl)	75.5 ± 12.3	42.0 ± 6.8*	28.8 ± 2.9	13.6 ± 1.9**
LDL cholesterol (mg/dl)	11.4 ± 0.4	19.4 ± 2.3*	31.8 ± 3.9$^{\#\#}$	53.8 ± 5.5
VLDL cholesterol (mg/dl)	6.3 ± 0.7	4.0 ± 0.4*	2.5 ± 0.2$^{\#\#}$	1.1 ± 0.3**
HDL cholesterol (mg/dl)	77.6 ± 4.8	95.9 ± 3.4*	115.3 ± 5.4$^{\#\#}$	123.4 ± 3.8

One-way ANOVA was performed to calculate statistical significance (*P < 0.05, **P < 0.01 vs control, $^{\#\#}P$ < 0.01 vs normal chow control).

Figure1

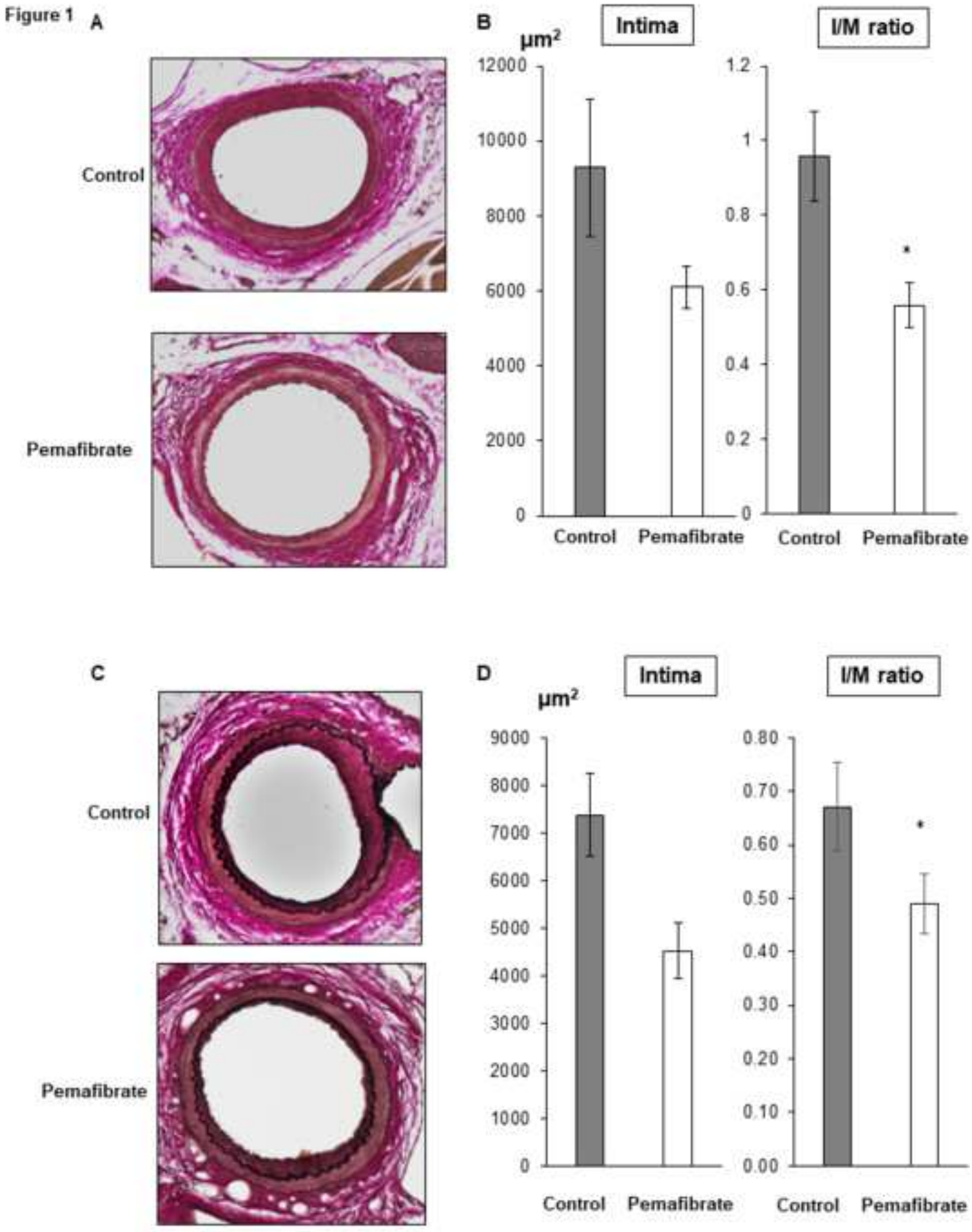
Figure 1
A
Control
Pemafibrate
B
Intima
μm²
12000
10000
8000
6000
4000
2000
0
I/M ratio
1.2
1
0.8
0.6
0.4
0.2
0
*
Control
Pemafibrate
Control
Pemafibrate
C
Control
Pemafibrate
D
Intima
μm²
9000
8000
7000
6000
5000
4000
3000
2000
1000
0
I/M ratio
0.80
0.70
0.60
0.50
0.40
0.30
0.20
0.10
0.00
*
Control
Pemafibrate
Control
Pemafibrate

Figure2

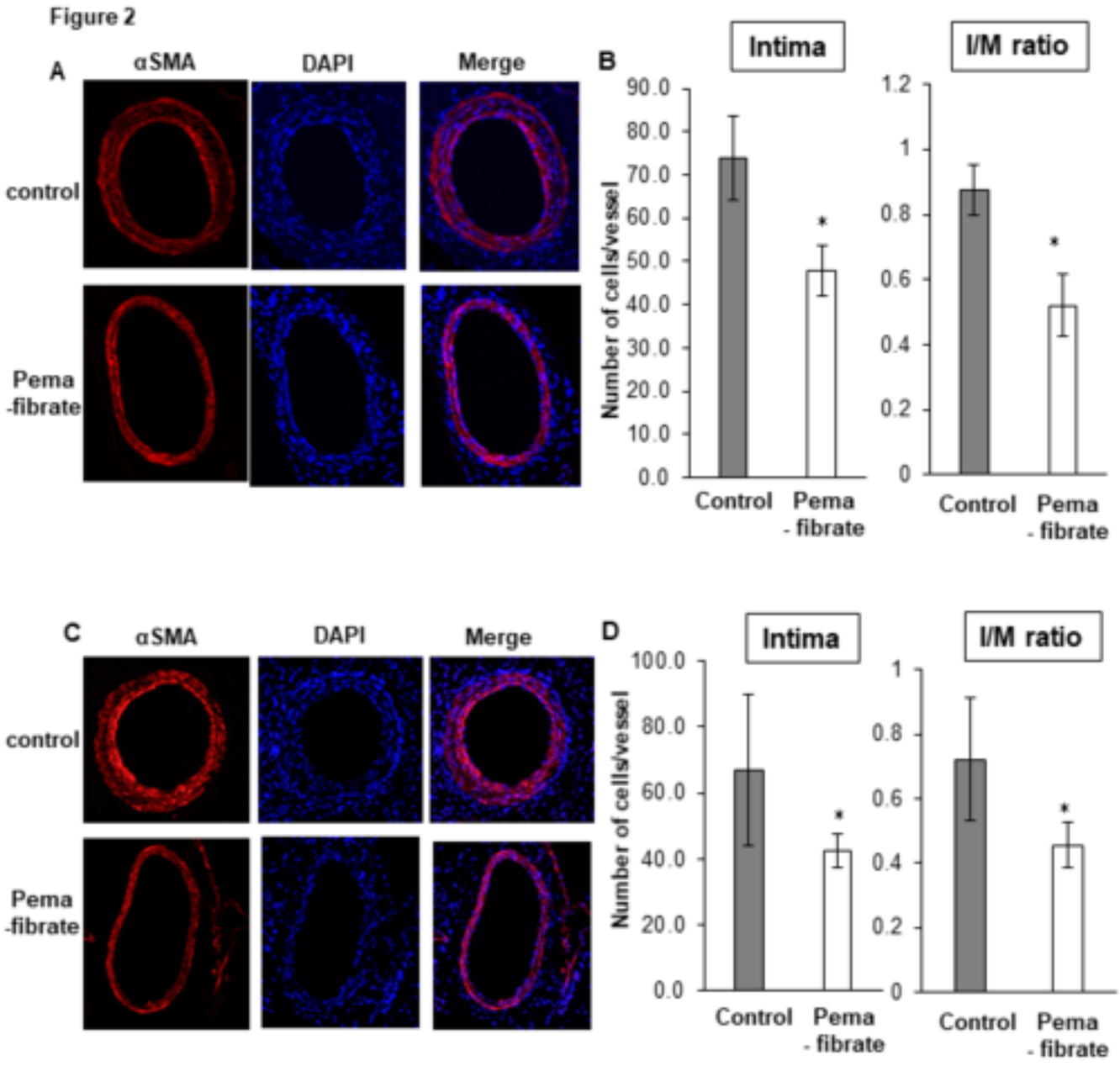
Figure 2
A
αSMA
DAPI
Merge
control
Pema
-fibrate
B
Intima
I/M ratio
Number of cells/vessel
90.0
80.0
70.0
60.0
50.0
40.0
30.0
20.0
10.0
0.0
1.2
1
0.8
0.6
0.4
0.2
0
*
Control
Pema
- fibrate
C
αSMA
DAPI
Merge
control
Pema
-fibrate
D
Intima
I/M ratio
Number of cells/vessel
100.0
80.0
60.0
40.0
20.0
0.0
1
0.8
0.6
0.4
0.2
0
*
Control
Pema
- fibrate

Figure3

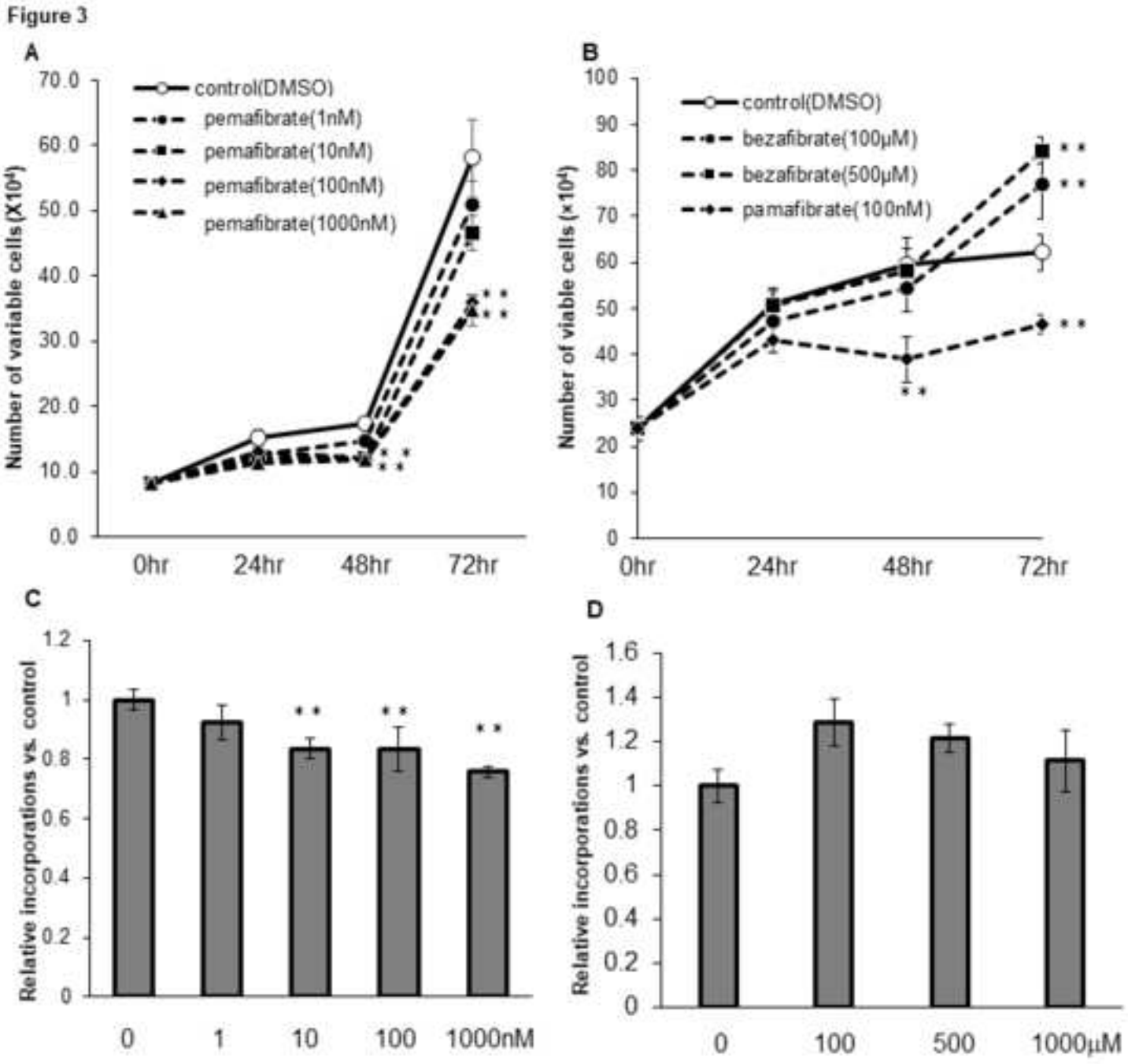
Figure 3
A
Number of variable cells (X10⁴)
70.0
60.0
50.0
40.0
30.0
20.0
10.0
0.0
control(DMSO)
pemafibrate(1nM)
pemafibrate(10nM)
pemafibrate(100nM)
pemafibrate(1000nM)
0hr
24hr
48hr
72hr
B
Number of viable cells (×10⁴)
100
90
80
70
60
50
40
30
20
10
0
control(DMSO)
bezafibrate(100μM)
bezafibrate(500μM)
pamafibrate(100nM)
0hr
24hr
48hr
72hr
C
Relative incorporations vs. control
1.2
1
0.8
0.6
0.4
0.2
0
0
1
10
100
1000nM
D
Relative incorporations vs. control
1.6
1.4
1.2
1
0.8
0.6
0.4
0.2
0
0
100
500
1000μM

Figure4

Figure 4

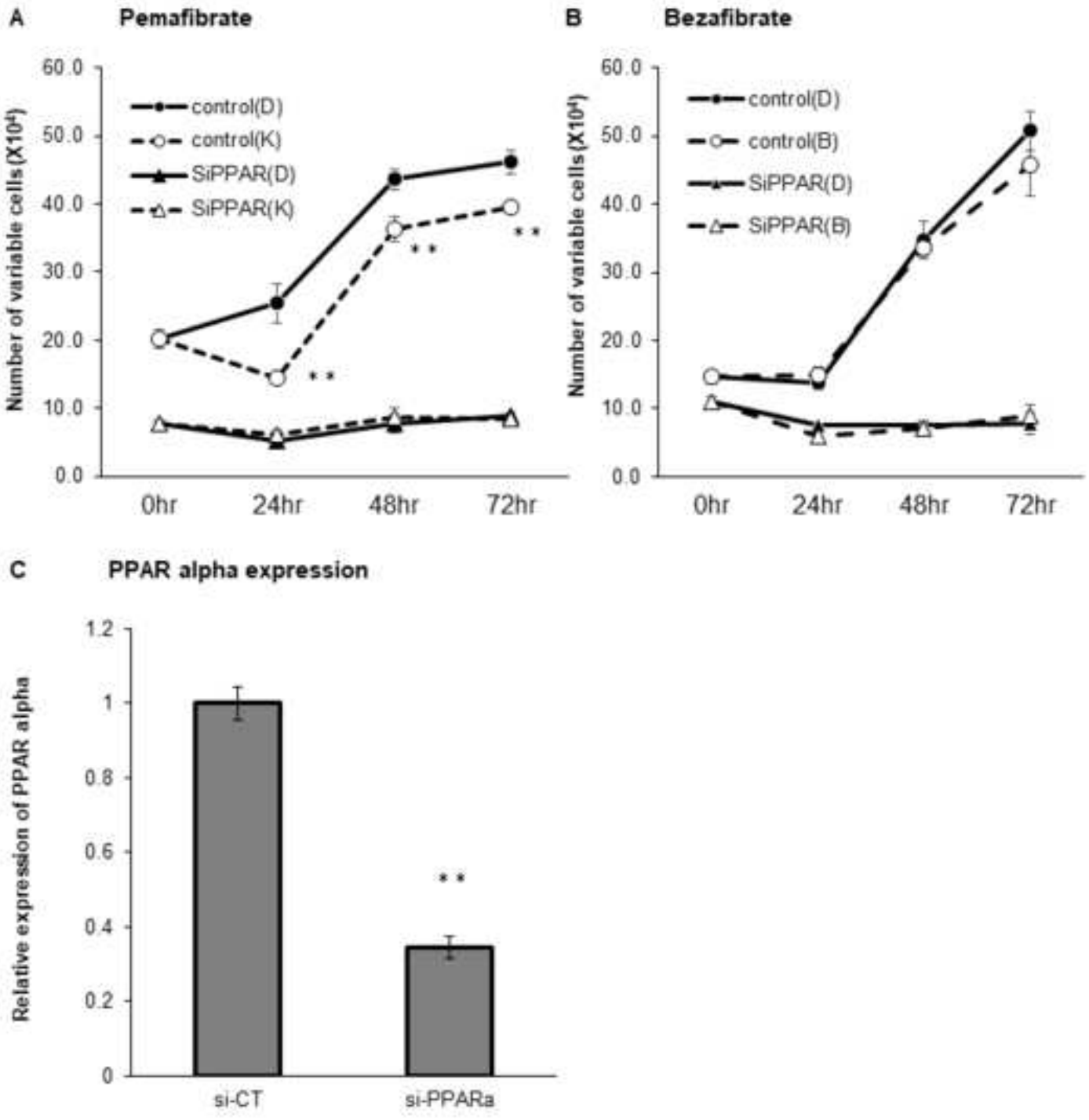

Figure5

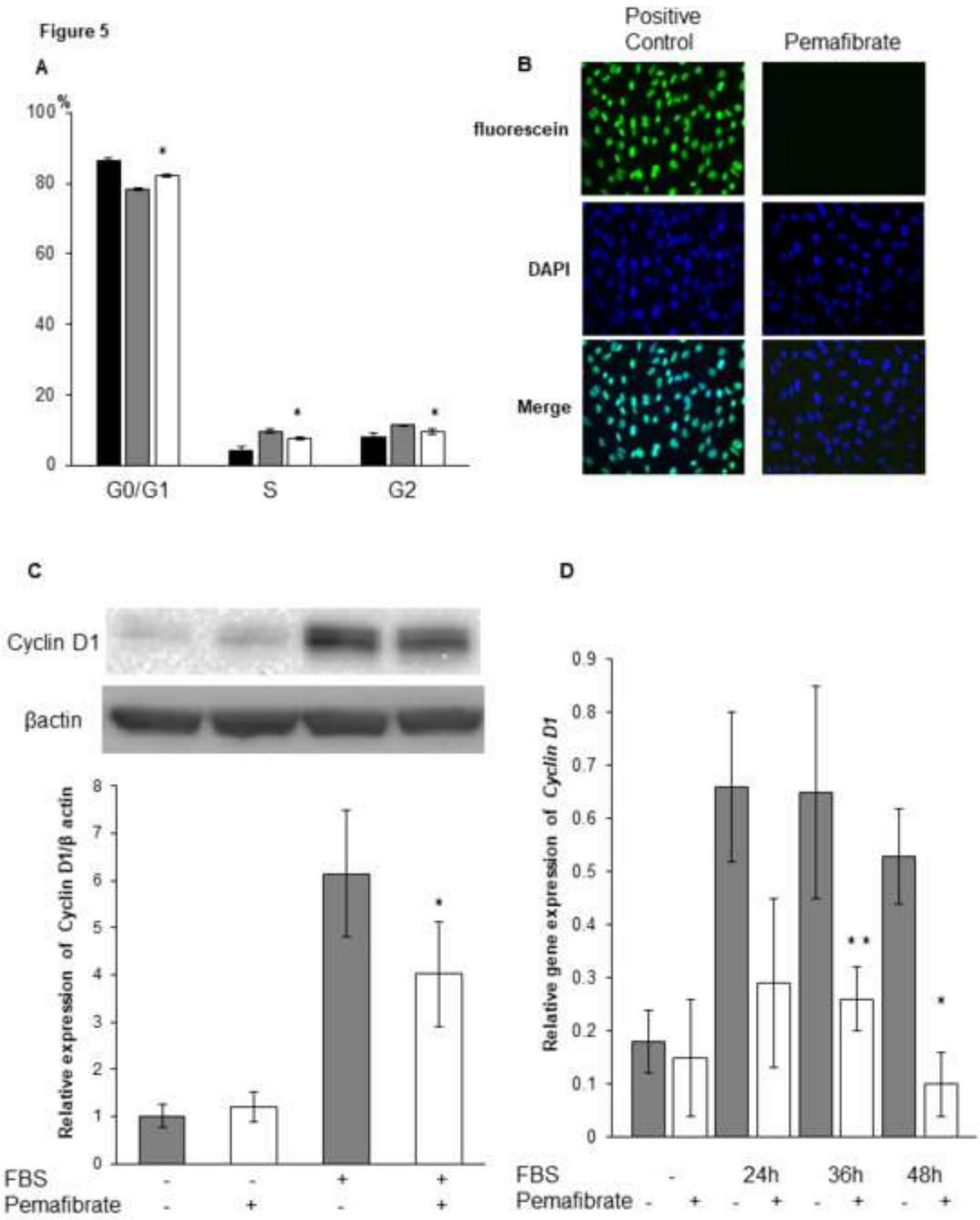
Figure 5
A
100 %
80
60
40
20
0
G0/G1
S
G2
B
Positive Control
Pemafibrate
fluorescein
DAPI
Merge
C
Cyclin D1
βactin
Relative expression of Cyclin D1/β actin
FBS
Pemafibrate
D
Relative gene expression of Cyclin D1
24h
36h
48h

Figure6

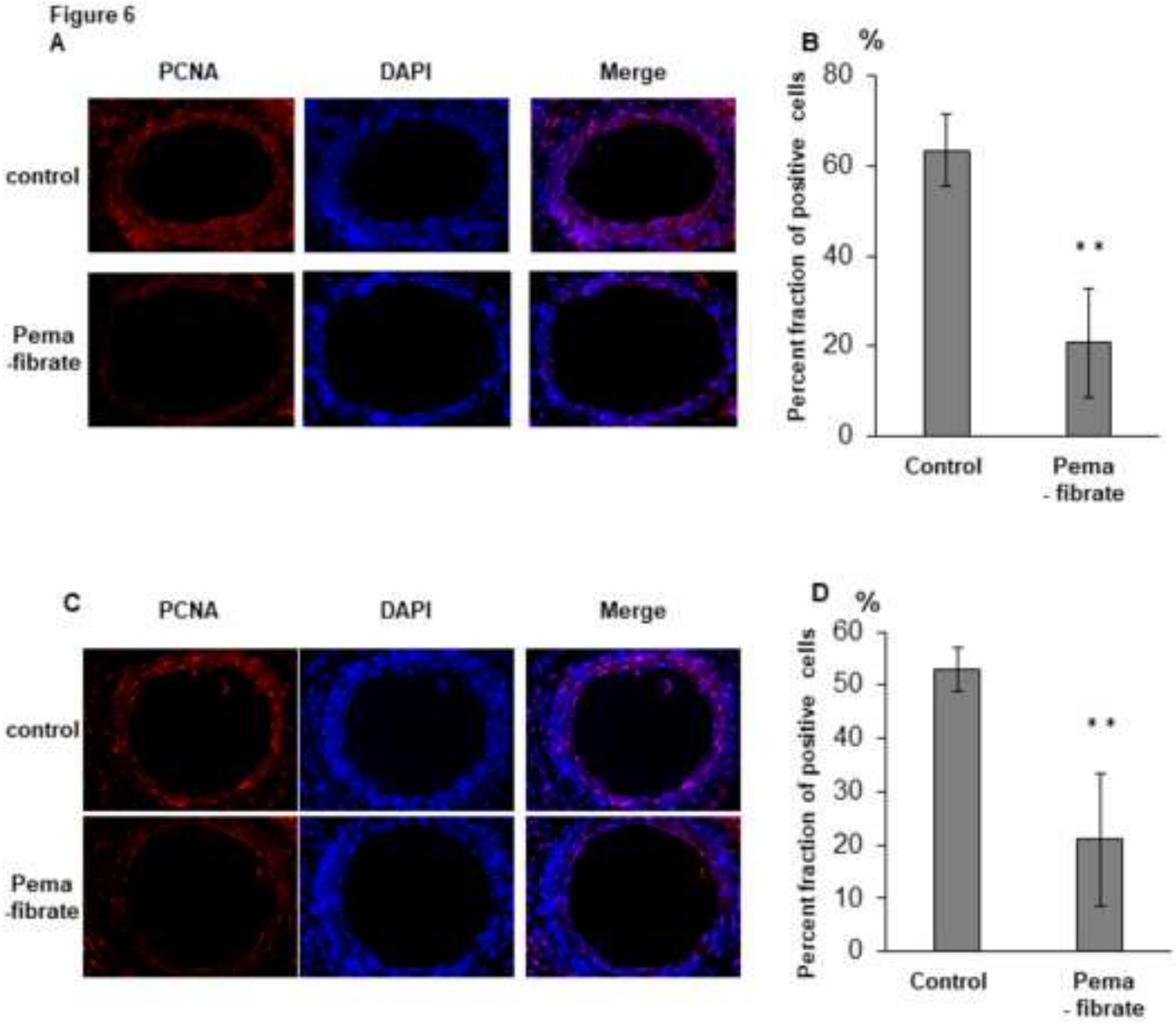
Figure 6
A
PCNA
DAPI
Merge
control
Pema
-fibrate
B
%
Percent fraction of positive cells
80
60
40
20
0
* *
Control
Pema
- fibrate
C
PCNA
DAPI
Merge
control
Pema
-fibrate
D
%
Percent fraction of positive cells
60
50
40
30
20
10
0
* *
Control
Pema
- fibrate